Leeside Flowfield and Heat Transfer of a Delta Wing at $M_\infty = 10$

K. Y. Narayan*
NASA Langley Research Center, Hampton, Va.

An experimental investigation was carried out to study the flowfield and heat-transfer characteristics of the leeside of an 80-deg swept delta wing at $M_\infty = 10$. Flow visualization studies were complemented by extensive heat-transfer measurements to obtain the details of the flowfield. Attached vortex-free flows and flows with inboard and leading-edge separation were observed. The dominant contributor to the heating load on the leeside is seen to be the vortices generated due to the boundary-layer separation, either at the leading edge or inboard. The experimental results also show that the angle of attack for incipient and leading-edge separation is strongly dependent on freestream Reynolds number.

Nomenclature

C_{pm} = model specific heat
M_∞ = freestream Mach number
R_∞ = freestream unit Reynolds number
$R_{\infty,x}$ = streamwise Reynolds number $(x \cdot R_\infty)$
$R_{\infty,l}$ = model length Reynolds number $(l \cdot R_\infty)$
$N_{St,\infty}$ = Stanton number based on freestream conditions
$N'_{St,\infty}$ = Stanton number normalized with the corresponding centerline value
$\dot{q}$ = heat-transfer rate
t = time
T_r = recovery temperature
T_w = wall temperature
x = coordinate along centerline from wing apex, positive downstream
α = angle of attack of lee surface
ρ_m = model density
ϕ = angle that a conical ray through apex makes with the centerline
ϕ_s = angle that the separation line makes with centerline
Λ = wing leading-edge sweepback angle
$\bar{\chi}$ = viscous interaction parameter $(M_\infty^3/\sqrt{R_{\infty,l}})$
λ_m = model skin thickness

Introduction

THE leeside flowfield of a delta wing at hypersonic speeds has received considerable attention in recent times, particularly as a research effort toward the development of the space shuttle. In spite of the number of investigations[1-5] that have been conducted over the years, our understanding of the leeside flowfield is still far from complete. A recent survey paper by Dunavant et al.[6] reviews the literature and highlights problem areas that need further investigation.

The dominant feature of the leeside flowfield (be it that of a simple delta wing, or cone, or the more complicated shuttle vehicle) is the presence of vortices in the flow. In general, the vortices are generated as a result of the interaction of the leeside boundary layer with the inboard compression field/oblique shock wave. The compression field/oblique shock wave is formed as the flow coming in from the leading edge turns to an axial direction in response to the flow coming in from the opposite leading edge. The details of the vortex flowfield, however, vary to a considerable extent, depending on the freestream and body geometrical parameters. Based on the details of the flow structure, the leeside flowfield of a delta wing can be classified as one of several types: 1) attached flows without any vortices, 2) attached flow with vortices embedded within the viscous layer, 3) flow attached at the leading edge but separated at the foot of the inboard shock wave, and 4) leading-edge separated flow. In the last case, the separated shear layer rolls up into a pair of conically growing vortices. In case 3, it has been suggested[7] that the separated shear layer rolls up also into a pair of conically growing vortices. Figure 1 shows schematically the different flow types.

Regardless of the manner of generation of vortices, however, the final outcome is increased heating (due to the stagnating cross flow) over the region of the wing where the vortices impinge on the surface. The generation of the vortices and their interaction with the lee surface is dependent on a number of parameters: 1) geometry of the wing, 2) angle of attack, 3) Mach number, 4) Reynolds number, and 5) a viscous interaction parameter. Each one of these has a characteristic and by no means small effect on the leeside flowfield.

In general, "embedded" vortices have been observed at moderate hypersonic Mach numbers, small angle of attack, and sufficiently large Reynolds numbers that the viscous interaction parameter $\bar{\chi} = M_\infty^3/\sqrt{R_{\infty,x}}$ is characteristically small [0(0.1)]. With increase in angle of attack, it is expected that this flow would change to the type with inboard separation and eventually to one with leading-edge separation. At higher Mach numbers, because of facility limitations, all of the existing measurements have been limited to fairly small Reynolds numbers, resulting in values of the viscous interaction parameters $\bar{\chi}$ of the order of one or more. Under these conditions, "embedded" vortices have not been observed. The types of flow which have been noted here are attached vortex-free flows, flows with inboard separations, and flows with leading-edge separation. Table 1 lists relevant

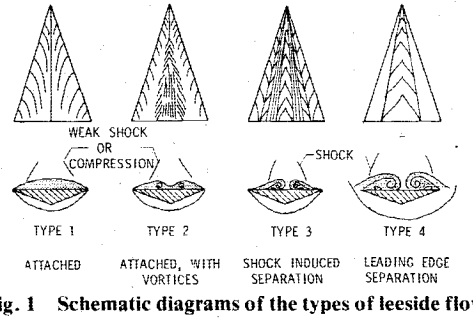

Fig. 1 Schematic diagrams of the types of leeside flow.

Presented as Paper 76-118 at the AIAA 14th Aerospace Sciences Meeting, Washington, D.C., Jan. 26-28, 1976; submitted March 10, 1977; revision received Oct. 6, 1977.

Index categories: Aerodynamic; Supersonic and Hypersonic Flow.

*NRC Resident Research Associate, Heat Transfer Section, Aerothermodynamics Branch, Space Systems Division; currently Scientist, Aerodynamics Division, National Aeronautical Laboratory, Banaglore, India. Member AIAA.

Table 1 Leeside flowfield investigations

Source	Λ, deg	M_∞	$R_\infty 10^{-6}$/m	χ	α, deg	Comments
Ref. 1	65, 70 75,78	6.0, 6.8	2-26	0.28-0.075	0-10	Heat transfer, static pressures, limited center-line pitot pressures, surface oil-flow and vapor screen visualizations. Embedded vortices observed at all α except α = 0 deg.
Ref. 2	75	10	2.4	1.5	0-50	Static pressures, pitot pressures, oil-flow and vapor screen visualizations. Did not observe embedded vortices.
Ref. 3	75	7	30	0.06	0-20	Static pressures, pitot pressures, oil flows, and vapor screen visualizations. Inboard separation occurs at α = 5 deg. Possible that embedded vortices exist for α < 5 deg.

data on some of the existing measurements. As Table 1 indicates, heat-transfer measurements are lacking at the higher Mach numbers. As a matter of fact, heat-transfer data do not seem available except at $M_\infty = 6$ or less. In this investigation, detailed surface heat-transfer data have been obtained for an 80-deg swept delta wing at $M_\infty = 10$. The experimental diagnostics consisted of surface oil-flow and vapor screen visualizations and static pressure† and heat-transfer distributions.

Experimental Details

The experiments were conducted in the $M_\infty = 10$ Continuous-Flow Hypersonic Tunnel at the Langley Research Center. The test conditions are summarized as follows: Mach number, 10.3; stagnation pressures, 3.45 and 9.65 MN/m^2; stagnation temperature, 970 K; Reynolds numbers, 2.2 and 6×10^6/m, respectively, corresponding to the two stagnation pressures (corresponding values of the viscous interaction parameter $\bar{\chi}$ are 1.46 and 0.88).

The vapor screen and some oil-flow tests were run with the tunnel cold. The test conditions in this case were Reynolds number of 2.3×10^7/m, calculated assuming the usual single-phase relations to be valid in the two-phase vapor/air-flow present, and $\bar{\chi} = 0.45$.

The model, an 80-deg swept delta wing with a flat lee surface and sharp leading edges, was sting-mounted on the incidence changing mechanism of the tunnel. The model could be pitched to a maximum of about 22 deg (referenced to the lee surface) before the tip went outside the test section core. The model had a centerline chord of 0.254 m.

The model could be run with one of three interchangeable plates. One of the plates was intrumented with a number of chromel alumel thermocouples. The thermocouples were located both on and off the centerline. Chordwise, they were located from 20 to 95% chord, whereas in the spanwise direction they were provided as close to the leading edge as possible. The second instrumented plate was provided with a limited number of static pressure orifices, whereas the third plate was not instrumented and used for oil-flow and vapor screen visualization tests.

Heat transfer was measured using the thin-skin calorimetry technique. In this technique, the rate of heat storage in the model skin is measured. The model, initially at room temperature, suddenly is injected into the test section of the tunnel after flow has been established, from a sheltered station outside. The model thus is subjected to a step input in the heat-transfer coefficient. The model is kept in the tunnel for about 5 to 7 s, during which time the temperature-time history is recorded. The data are converted into heat-transfer coefficients using the equations

$$\dot{q} = \rho_m C_{p_m} \lambda_m \frac{dTw}{dt}$$

$$h = \dot{q}/(T_r - T_w)$$

Oil-flow patterns were obtained by covering the model with random droplets of a mixture of lampblack and silicone oil. The model was injected into the test section after flow was established and visually monitored during the run. It was retracted from the test section when a stable pattern was formed and the results photographed. In general, about 20 to 30 s were required for a stable pattern to be formed.

Results: Flow Visualization

Typical oil-flow patterns are shown in Fig. 2, whereas the vapor screen visualizations (at $X = 0.2$ m) are shown in Fig. 3. In interpreting the oil-flow patterns, we follow Maskell's[8] definition that a three-dimensional separation line is an envelope of converging limiting surface streamlines. In many three-dimensional situations under marginal shear conditions, oil may accumulate along a line because the surface shear becomes too low to overcome the friction and surface tension

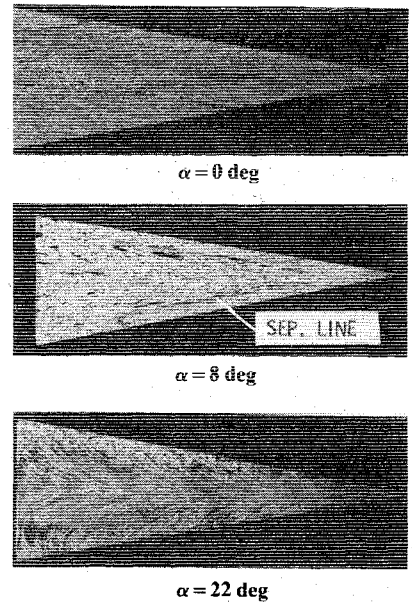

α = 0 deg

α = 8 deg

α = 22 deg

Fig. 2 Oil-flow patterns (Λ = 80 deg, $M_\infty = 10.3$, $R_\infty = 2.2 \times 10^6$/m).

†Although the static pressures were measured at a number of stations on the surface of the model, the coverage was not fine enough for a meaningful discussion of the results. Thus, the pressures have not been presented in this paper, but use has been made of them to calculate the heat transfer on the wing.

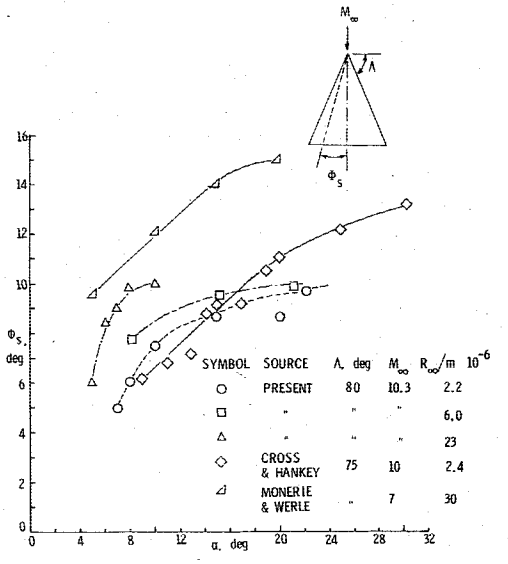

Fig. 3 Separation line location.

Fig. 4 Vapor screen visualizations ($\Lambda = 80$ deg, $M_\infty = 10.3$, $R_\infty = 23 \times 10^6$/m, $X = 0.2$ m).

of the oil droplets. One should be careful not to interpret this anomalous accumulation line as a separation line. The true separation line would, in the Maskell sense, have streamlines converging on it from either side.

An examination of the oil-flow patterns indicates three (of the four listed earlier) different flow types: 1) attached flow without any vortices, 2) flow attached at the leading edge but separated inboard and subsequently reattaching at the centerline, and 3) flow separated at the leading edge and reattaching at the centerline.

Attached flow occurs at $\alpha = 0$ deg at all three Reynolds numbers and at $\alpha = 5$ deg at the smallest Reynolds number (2.2×10^6/m). The surface streamlines show an inflow from the leading edge and a gradual turning to the axial direction further inboard. The flow can be considered to be quasi-two-dimensional and, under certain conditions (which will be elaborated on at a later stage), is amenable to a strip theory calculation.

Inboard separation is identified by the presence of an oil-accumulation line with streamlines converging from both sides. From the oil-flow patterns, it was seen that the first appearance of separation (incipient separation) occurs at lower angles of attack at higher Reynolds numbers. As the angle of attack is increased beyond that required for incipient separation, the separation line moves outboard, eventually reaching the leading edge. Again, the angle of attack at which separation first reaches the leading edge is a fairly strong function of unit Reynolds number, an increase in Reynolds number causing an earlier leading-edge separation.

The separation line exhibits a nonconical behavior by turning outboard toward the wing tip close to the trailing edge. Furthermore, the beginning of the nonconical behavior seems to move upstream with increase in angle of attack. This suggests that the nonconical effect is base-flow induced (because of the pressure gradient of the wake recompression shock). The meridional region appears to be unaffected by the presence of the wake recompression shock because the high-shear, reattached flow in that region is better able to negotiate the adverse pressure gradient associated with the shock. Cross and Hankey[2] also noted this nonconical behavior of the separation line, and, as a matter of fact, their results showed that, for $\alpha \geq 20$ deg, an extensive region of base-flow-induced separation was present.

The location of the separation line (ϕ_s, measured from the oil-flow patterns) relative to the wing centerline is plotted in Fig. 3 as a function of the angle of attack at the three unit Reynolds numbers. The results of Cross and Hankey[2] at a Mach number of 10 and Monnerie and Werle[3] at a Mach number of 7, both on a wing of 75-deg sweep-back angle, also are plotted in the figure for comparison. Both of these measurements show a linear variation of ϕ_s with α up to some angle of attack, whereas the present measurements show a considerably nonlinear variation of ϕ_s over the entire α range. The Reynolds number effect on the location of separation mentioned earlier is brought out clearly in the figure, where it is seen that, at any angle of attack greater than that for incipient separation, the separation line lies outboard at the higher Reynolds number. Cross and Haney's[2] measurements at two Reynolds numbers ($R_{\infty,\ell} = 2.76 \times 10^5$ and 4.28×10^5) do not show any noticeable variation of ϕ_s.

The Reynolds number dependence of ϕ_s can be explained on the basis of the variation in the boundary-layer thickness close to the leading edge. The boundary-layer displacement thickness decreases with increase in Reynolds number; thus the effective flow expansion at the leading edge is larger at the higher Reynolds number. This increases the strength of the inboard oblique shock wave, which turns the flow to the axial direction, and thus separation is expected to occur at a smaller angle of attack at higher Reynolds numbers.

Two other points regarding inboard separation are worth mentioning at this stage. The first point is that, at incipient separation, the separation line is inclined at an angle (to the centerline of the wing) that is roughtly equal to the freestream Mach angle. This has been observed at all of the three Reynolds numbers and also has been noted by Cross and Hankey.[2] We believe that separation should occur first slightly outboard of a ray inclined at the local Mach angle (since, in inviscid flow, the inboard oblique shock wave would lie along the local Mach line through the wing apex). Thus the fact that separation first occurs along the freestream Mach

line through the apex is nothing more than an interesting coincidence and may not be expected to be a general result.

The second point concerns the angle of attack at incipient separation. Reding and Ericsson,[9] based on the measurements of Cross and Hankey[2] and also some measurements on a delta wing orbiter, pointed out that incipient separation occurs at the angle of attack at which the windward side shock detaches from the leading edges. This also need not be generally valid, since, if true, it implies that 1) if the shock wave is detached, there is inboard separation on the leeside, and 2) inboard separation is Reynolds-number independent. Neither of these points is supported by the present measurements. The shock wave is detached at all incidences (because of the large leading-edge angle on the windward side), but inboard separation does not occur until $\alpha = 7$ deg (at $R_\infty = 2.2 \times 10^6$/m), and, furthermore, the present results show a considerable Reynolds number effect.

The vapor screen photographs at a streamwise location, $\chi = 0.5$ m, at $R_\infty = 2.3 \times 10^7$/m are shown in Fig. 4. At $\alpha = 0$ deg, the vapor screen shows the characteristic piling up of the viscous fluid in the meridian plane. This is due to the viscous-interaction-induced pressure at the leading edge feeding low-energy boundary-layer fluid into the meridional region. At $\alpha = 5$ deg, however, the viscous layer has a "flat-top" shape close to the apex at a "trough" at the meridian further downstream. This behavior of the viscous-layer thickness at the lee meridian is consistent with the presence of a vortex in the viscous-layer scavenging fluid from the meridional region.

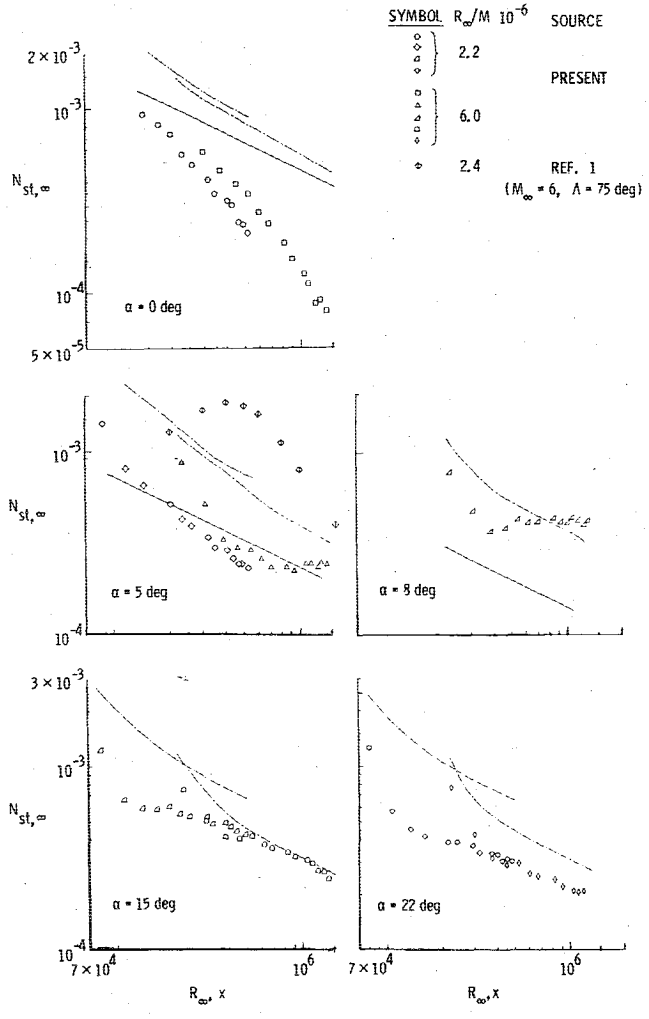

Fig. 5 Centerline heat-transfer variation (——, strip theory calculation with P-M pressures; – – –, strip theory calculation with measured pressures, $R_\infty = 6 \times 10^6$/m; —·—, strip theory calculation with measured pressures, $R_\infty = 2.2 \times 10^6$/m).

Although the vortices seem to be "embedded" in the viscous layer, the vortex generation here involves boundary-layer separation (as the oil-flow patterns show), and, thus, the flowfield is different from the "embedded" vortex-type flow observed by Rao and Whitehead[1] at $M_\infty = 6$. At higher angles of attack, the vapor screen pictures show only that the viscous region has increased in extent; no other details can be noted.

Heat-Transfer Distributions

The centerline and spanwise heat-transfer distributions are presented in Figs. 5 and 6 in the form of Stanton number $N_{St,\infty}$ based on freestream conditions. Laminar heat-transfer rates calculated using the strip theory (based on Monaghan's T' method[10]) also are plotted in some of the figures for comparison. Although the calculated values may not be expected to be in strict accord with the measurements, they are useful landmarks in discussing the experimental results.

At $\alpha = 0$ deg, the measured Stanton numbers on the centerline are much smaller than the corresponding calculated two-dimensional values and further decrease much more rapidly than the $R_{\infty,x}^{-1/2}$ variation of the theory. The large difference between the measurement and the estimation is due to the high viscous-interaction-induced pressures [$\bar{\chi} = 0(1)$] near the leading edge feeding low-energy boundary-layer fluid to the meridional region, thus causing a piling-up of the low-energy fluid there. The results also show a unit Reynolds number effect, the Stanton number being higher at the higher Reynolds number. This also is presumably due to the stronger viscous interaction at the lower Reynolds number. Rao and Whitehead's[1] measurements at $M_\infty = 6$ and $\bar{\chi} \approx 0(\cdot 1)$ were, on the other hand, in good accord with the calculated two-dimensional laminar (and turbulent) boundary-layer values because of the much smaller viscous interaction.

The spanwise heat-transfer variation (normalized by the centerline value), Figs. 6 and 7, shows the expected behavior; i.e., the heat transfer is a minimum at the centerline and

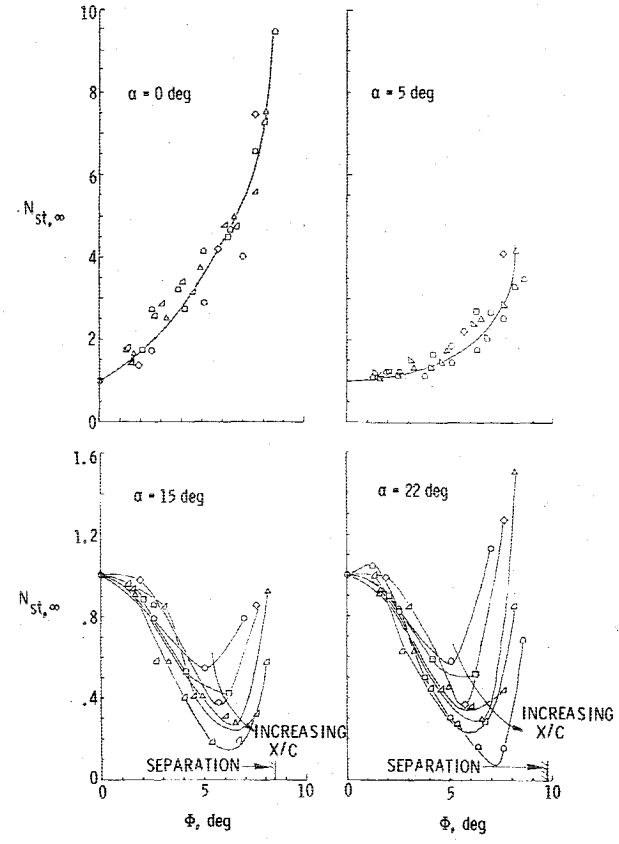

Fig. 6 Spanwise heat-transfer variation ($R_\infty = 2.2 \times 10^6$/m). Lines are faired through experimental points.

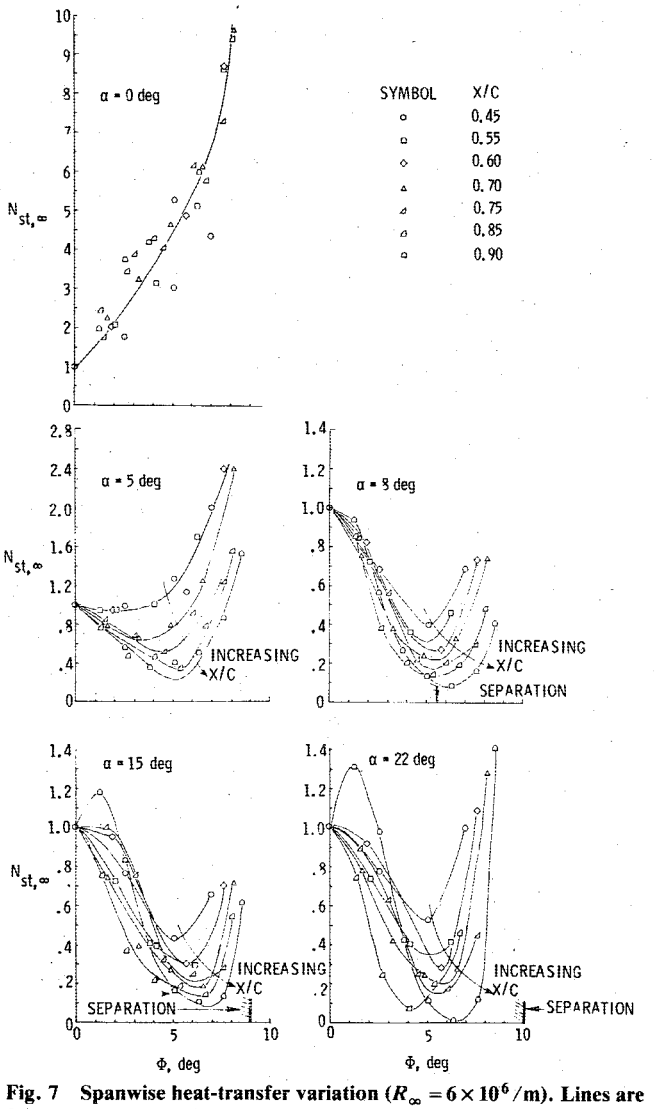

Fig. 7 Spanwise heat-transfer variation ($R_\infty = 6 \times 10^6$/m). Lines are faired through experimental points.

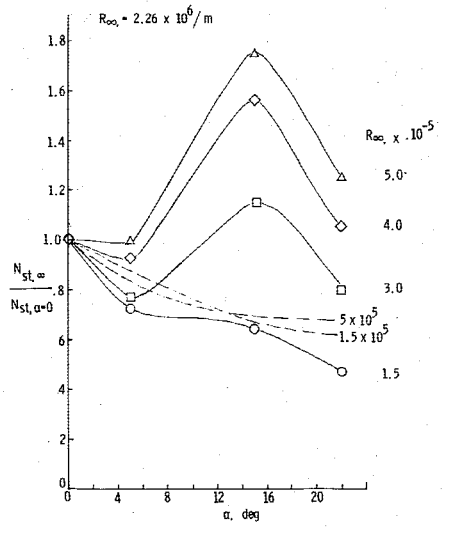

Fig. 8 Centerline heat-transfer excursions with angle of attack ($R_\infty = 2.2 \times 10^6$/m; ——, faired through experimental points; ---, strip theory calculations using measured pressures).

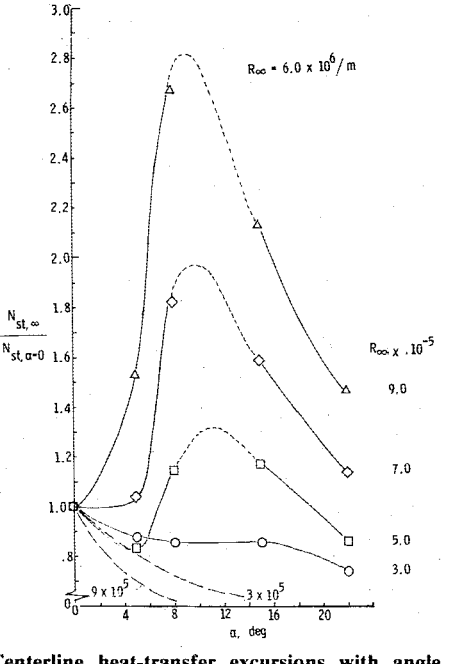

Fig. 9 Centerline heat-transfer excursions with angle of attack ($R_\infty = 6 \times 10^6$/m; ——, faired through experimental points; ---, strip theory calculations using measured pressures).

increases rather sharply toward the leading edge. Stanton numbers at different streamwise stations correlate in terms of the ray angle ϕ. It should be pointed out, however, that the flow is not conical, since the heat-transfer rate varies considerably along conical rays from the apex, as the centerline results show. The results also show a unit Reynolds number effect, the heat transfer at the higher Reynolds number being higher than at the lower number.

As the angle of attack is increased beyond $\alpha = 0$ deg, the centerline heat-transfer distributions (Fig. 5) do not show the kind of peak observed by Rao and Whitehead.[1] Since the two sets of measurements at $\alpha = 5$ deg span the same streamwise Reynolds number range, the large differences between the two is due to the difference in freestream Mach number (or, equivalently, in the viscous interaction parameter $\bar{\chi}$). Of course, the difference of 5 deg in the sweepback angle would not be expected to contribute significantly to the differences between the two sets of results.

The level of heat-transfer rate for $\alpha = 5$ deg is generally lower than the strip theory estimates (Fig. 5), except at $\alpha = 15$ deg, where the agreement between the measurement and estimation is surprisingly good. This agreement would seem to be fortuitous, since the oil-flow pattern at this α shows a strong outflow from the centerline, making the quasi-two-dimensional assumption rather dubious.

The character of the spanwise heat-transfer distribution (Figs. 6 and 7) changes from one with a minimum on the meridian in attached flow to one with a peak on the meridian and a minimum between the meridian and the leading edge for inboard and leading-edge separated flows. This change in the character of the spanwise heat-transfer variation correlates with the appearance of the separation line in the oil-flow patterns. There is no notable feature in the heat-transfer distributions readily distinguishing inboard separation from leading-edge separation. However, the trough in the heat-transfer rate appears to move outboard by a small amount with the outboard movement of the separation line.

The location of the separation line measured from the oil-flow patterns is shown in the spanwise heat-transfer distributions (Figs. 6 and 7). Unfortunately, except at $\alpha = 8$ deg, the separation lies outboard of the last measurement station. However, as the results at $\alpha = 8$ deg show, the heat-transfer distribution does not have any notable feature at the separation point. In this connection, it may be pointed out that, in two-dimensional separated flows, the separation point is not the point of minimum heat transfer.

The excursions of the centerline heat-transfer rate over the angle of attack range are shown in Figs. 8 and 9. In the absence of vortices in the flow, the heat transfer at any Reynolds number would decrease continuously with angle of attack, as the strip theory calculations indicate. An increase in heat transfer with α is thus evidence of the presence of vortices. This still does not tell us whether the vortices are generated in the manner of Rao and Whitehead's[1] model (embedded vortices) or generated as a result of boundary-layer separation. However, the oil-flow patterns in these cases show unmistakable evidence of separation, and thus we can conclude that the vortex generation is a consequence of separation and reattachment. The data at $R_{\infty,x} = 9 \times 10^5$ show an increase in heat transfer for $\alpha > 0$ deg, but the oil flow for this condition does not indicate separation until $\alpha = 5$ deg. It is possible that a pair of weak vortices generated in the manner of Rao and Whitehead's[1] model might be embedded in the viscous layer. The embedded vortices might be too weak and be situated at a distance from the wing surface so as not to leave a footprint on the surface. The decrease in heat transfer beyond the peak is due to the weakening of the vortices as the local Mach number increases with angle of attack.

A point of interest is the qualitative similarity in the $N_{ST}/N_{St,\alpha=0}$ vs α plots between delta wing, cone, and shuttle orbiter. Figures 6 and 13 of Ref. 6 show such plots for the cone and the orbiter, respectively, and the similarity between these results and the present one on a delta wing is fairly obvious.

Conclusions

Detailed surface flow visualization and heat-transfer data have been obtained on the lee surface on an 80-deg swept-back delta wing at $M_\infty = 10$. Attached, inboard separated and leading-edge separated flows were observed, and the surface flow and heating characteristics of each type has been catalogued. The strong dependence of the boundary between these different flow regimes on the freestream Reynolds number has been shown and the dependence explained qualitatively. Further work, mainly in the form of extensive flowfield probing, is necessary to obtain a full understanding of the vortical flow on the lee surface.

The measurements do not seem to indicate large differences in the heat-transfer characteristics between the inboard separated case and the leading-edge separated case. The only notable difference is the small outboard movement of the heat-transfer minimum in response to a similar movement of the separation line. The surface flow at the lee meridian seems to be unaffected as the separation moves toward the leading edge, pointing to a general similarity between the two flow types.

Acknowledgment

The author acknowledges J. C. Dunavant, Space Systems Division, and D. M. Rao, Subsonic-Transonic Aerodynamics Division, Langley Research Center, for many interesting discussions.

References

[1] Rao, D. M. and Whitehead, A. H., Jr., "Lee-Side Vortices on Delta Wings at Hypersonic Speeds," *AIAA Journal*, Vol. 10, Nov. 1972, pp. 1458-1465.

[2] Cross, E. J., Jr. and Hankey, W. L., "Investigation of the Lee-Ward Side of a Delta Wing at Hypersonic Speeds," *Journal of Spacecraft and Rockets*, Vol. 6, Feb. 1969, pp. 185-190.

[3] Monnerie, B. and Wele, H., "Etude de L'ecoulment Supersonique et Hypersonique Autuor d'une Aile Elancee en Incidence," AGARD C.P. 30, 1968.

[4] Whitehead, A. H., Jr., "Effects of Vortices on Delta Wing Lee-Side Heating at Mach 6," *AIAA Journal*, Vol. 8, March 1970, pp. 599-600.

[5] Whitehead, A. H., Jr. and Keyes, J. W., "Flow Phenomena and Separation Over Delta Wings with Trailing-Edge Flaps at Mach 6," *AIAA Journal*, Vol. 6, Dec. 1968, pp. 2380-2387.

[6] Dunavant, J. C., Narayan, K. Y., and Walberg, G. D., "A Survey of Leeside Flow and Heat Transfer on Delta Planform Configurations," AIAA Paper 76-118, Washington, D.C., 1976.

[7] Stanbrook, A. and Squire, L. C., "Possible Types of Flow at Swept Leading Edges," *Aeronautical Quarterly*, Vol. 15, Part 1, Feb. 1964, pp. 72-82.

[8] Maskell, E. C., "Flow Separation in Three Dimensions," Royal Aircraft Establishment, England, Rept. Aero. 2565, Nov. 1955.

[9] Reding, J. P. and Ericsson, L. E., "Review of Delta Wing Space Shuttle Vehicle Dynamics," Paper 30, NASA TM X-2508, 1972.

[10] Monaghan, R. J., "An Approximate Solution of the Compressible Laminar Boundary Layer on a Flat Plate," Aeronautical Research Council, England, R&M 2760, 1953.